

Modeling the passive cardiac electrical conductivity during ischemia

Jeroen G. Stinstra, Shibaji Shome, Bruce Hopenfeld and Rob S. Macleod

Abstract—A geometrical model of cardiac tissue was used to compute the bidomain conductivities. We simulated ischemic conditions by adapting the geometrical model to morphological and electrical changes reported in literature. The simulated changes included 1) expansion of capillaries 2) cell swelling and 3) the closure of gap junctions, which coincide with changes associated with the three phases of ischemia reported in the literature. Simulations were carried out in a finite element model describing 64 myocytes and the apparent conductivity was calculated by computing the amount of current in this piece of tissue due to an externally applied electric field. In the first case, capillary swelling led to a reduction in extracellular longitudinal conductivity by about 20%, which is in the range of reported literature values. Moderate cell swelling did not affect extracellular conductivity considerably. In order to match the reported drop in total tissue conductance in experimental studies during the third phase of ischemia, we simulated a ten fold increase in gap junction resistance. This ten fold increase correlates well with the reported changes in gap junction densities in literature.

Keywords—Conductivity, Cardiac tissue, Bidomain, Ischemia, Cardiac modeling

I. INTRODUCTION

Ischemia is a state in which cells are receiving abnormally low amounts of nutrients. Ischemia in the heart is typically caused by the partial or complete blockage of a coronary artery and is a precursor to a host of changes in cardiac tissue properties. Primary changes include alterations in myocyte [19] and vascular morphology [11] and gap junction resistance [3]. Somewhat less significant changes occur in the conductivity of the interstitial space as a result of changes in the concentration of potassium ions due to ischemia [23].

Although there is substantial uncertainty regarding the effect of ischemia on conductivity, there appear to be three phases of conductivity changes: (1) immediately upon perfusion arrest, there is a substantial and sharp increase in longitudinal extracellular resistance [11], [15]; (2) after perfusion arrest, a more gradual rise in longitudinal extracellular resistance lasting for at least 15 minutes [23]; and (3) overlapping with the second phase, a rapid rise in longitudinal intracellular resistance approximately 15–30 minutes after perfusion arrest [10], [11], [15].

The above observations seem to agree with studies reporting measurements of whole tissue (bulk) resistance during ischemia [4], [13]. In these studies, although different species were used, and ischemia was sustained for different time periods, the change of bulk resistance in time is similar.

Previous findings suggest several possible mechanisms for these three phases of ischemia induced conductivity changes.

Following the arrest of coronary flow an immediate increase in the extracellular longitudinal resistance by about 30% has been observed [11]. Kléber *et al.* proposed that this increase is due to the collapse of capillaries after cardiac arrest. However measurements by Fleishhauer *et al.* [6] suggest that the capillary system does not contribute to the overall extracellular conductivity and thus a change in capillary volume would not alter the extracellular conductivity. The simulations in this report will show that the conductivity of the capillary system is substantially lower than that of the interstitial space, because transverse currents have to pass in and out of the capillaries through a highly resistive capillary wall and longitudinal currents have to flow around numerous red blood cells that almost completely clog the capillaries. Hence, we propose an alternative mechanism, namely that the immediate increase in longitudinal resistivity during the first phase is caused by a small but rapid decrease in the size of the interstitial space as fluid shifts from that space into the capillaries because of the decrease in capillary hydrostatic pressure directly after perfusion arrest.

The second phase, during which there is a more gradual rise in extracellular longitudinal resistance [15], occurs as a result of cell swelling, which initially decreases the volume of the interstitial space as fluid from there flows into the myocytes [23]. After the osmotic balance between the cell and the interstitial space is reestablished, both the cell and the interstitial space may swell, with water being divided between those spaces according to their respective volumes, as the higher osmolality of the interstitial space draws water from more distant, non-ischemic parts of the heart [19]. The proportional increase in both the intracellular and interstitial volumes probably does not greatly alter the bidomain conductivities. The extent of cell swelling may depend on whether the ischemia is low flow or no flow. In the case of no flow ischemia, metabolite washout is minimal, so interstitial osmolyte accumulation at least partially balances intracellular accumulation and only modest increases in cell volume may occur [22]. In low flow ischemia, in contrast, washout of interstitial osmolytes would maintain an osmotic imbalance between the interstitial and intracellular spaces, resulting in greater swelling [22].

The third phase of resistance changes, a rapid increase in intracellular resistance, is likely attributable to the closing of gap junctions [10], [13], [15]. According to Beardslee *et al.* [1], about 15 minutes after blocking perfusion to the myocardium, a considerable dephosphorylation of Connexin-43 takes place, which leads to the closure of gap junctions. Furthermore, it was shown that prolonged ischemia in isolated rabbit hearts resulted in doubling of intracellular calcium

concentration and a drop in intracellular pH to about 6.0 before a sharp rise in the bulk tissue resistance was observed [13]. A recent study on cultured mouse astrocytes showed a correlation between prolonged intracellular acidification with the decoupling and internalization of Connexin-43 [5]. These results can be extrapolated to the cardiac domain, since cardiac tissue also contains Connexin-43, and thus supports the hypothesis that the sharp rise in intracellular resistance is correlated with gap junction uncoupling.

Experimental studies have shown that the time of onset of different phases of arrhythmia correlate in time with onset of changes in tissue impedances. A common way of studying the origin of arrhythmias in a three dimensional substrate of myocardium, is by using a computer model simulating the effect of changes in the substrate. However these models are primarily based on changes in the driving currents within and across the myocyte membrane. One of the effects that is commonly not taken into account in these models, are the electrical conductivity changes that occur in ischemic cardiac tissue. Cell swelling and the decoupling of gap junctions alter the microscopic structure of tissue and hence its passive electrical conductivity. This change in conductivity will influence the volume conduction problem and thus change the epicardial potentials. A recent modeling study by Hopenfeld *et al.* [9] showed that the electrical anisotropy of cardiac tissue is a prime determinant of the distribution of epicardial potentials and changes in anisotropy will be reflected as changes in potential distributions.

The difficulty of modeling the changes in passive electrical properties lies in estimating the conductivity values of ischemic tissue, as measurements are sparse and are often hard to interpret. Moreover models are often based on the bidomain equations which split the conductivity tensor into two parts, an extracellular and an intracellular contribution. However, most conductivity measurements even under ischemic conditions always measure a weighted average of both tensors. Hence in order to separate them out, a modeling approach is always needed and additional structural information needs to be fed into those equations to obtain realistic values for the bidomain conductivity tensors.

In a related study [17], we created a geometrical model of cardiac tissue under healthy conditions to compute the conductivity of cardiac tissue. This model describes the geometry of cardiac tissue at a cellular level and computes the currents flowing at this microscopic level. Based on this information the average conductivity of a piece of tissue can be determined. The aim of this paper is to present the results of this model when we assume ischemic conditions and to compare them with the sparse measurements found in literature.

II. METHODS

In the next paragraph a brief description of the model is presented and subsequent changes needed to simulate the conductivity under ischemic conditions.

A. The conductivity model

The model used to compute the effective passive conductivity of cardiac tissue is based on a geometrical model of

a piece of cardiac tissue described at a cellular level. The model consists of two domains, the intracellular space of the myocytes (ICS) and the extracellular space surrounding the myocytes (ECS), separated by the cell membrane. Previous simulations suggested that the resistance of the capillary network is significantly different from that of the interstitial space [17], hence the ECS domain was subdivided into these two compartments. Similarly the ICS domain was divided into a compartment of intracellular fluid and one representing the gap junctions connecting the various myocytes. The conductivities of both the intracellular and extracellular fluids are assumed to be homogeneous and ohmic. In the model, the myocytes dimensions are roughly 10 by 25 by 100 μm and all the cells have their long axis aligned along the same longitudinal fiber direction.

The actual geometrical model itself was generated using a computer algorithm, that assigns a rule-based random-shape to each myocyte in the model. The goal of this program was to scrutinize the dependence of the model on general tissue properties, such as cell size and the overall size of the extracellular space and not to depend on the actual shape of every individual myocyte. Simulations under healthy conditions already demonstrated that the apparent conductivity is more dependent on the "global" tissue properties than on the actual shape of each myocyte. Hence we used the same approach for ischemic tissue. Each set of global parameters is an average of the results of ten different cellular layouts that were randomly generated. In the latter case it is only the difference of the individual cell shapes that have been changed, the overall properties of the tissue such as average cell-to-cell distance and overall volume fractions are kept the same.

[INSERT FIGURE 1]

The process of generating the tissue mesh is shown in Figure 1. This figure depicts the process of turning a regular mesh consisting of hexahedral elements into a model of myocytes embedded in an extracellular mesh of interstitial space and capillaries. The figure briefly depicts how myocyte shapes are generated that mimic the spiky elongated shapes typically seen in microscopic images of myocytes [7]. Depicted in the figure as well, is a small illustration of where the gap junctions are generated in the model. In our model we assume that the spiky processes of the myocytes connect one myocyte to the next myocyte by means of gap junctions. A recent study by Jain *et al.* [10] using confocal microscopy showed a similar distribution of gap junction proteins. The model is created in such a way that its processes along the fiber direction all touch each other (no layer of interstitial space is in between). Based on measurements of cell-to-cell resistivities we estimated a surface resistance that connects both cells. The latter is the model we used for the gap junctions. A more complete overview of this model can be found in [17].

The inhomogeneities in the extracellular space stem from the division into capillaries and interstitial space. Because at these microscopic scales, blood is not a homogeneous medium, its composition of red blood cells and blood plasma must be taken into account. Measurements of the conductivity of blood at different haematocrit levels indicate that the red cells do not conduct and that the blood plasma is the conductive

medium [20]. As the size of a red blood cell is approximately equal to the cross section of a capillary, it will block the conducting pathway along the capillary. In the model we constructed, each capillary has been split into three sections, the capillary wall, the blood cells and the blood plasma. We assumed a haematocrit of 50 % so that an essentially non-conductive red blood cell blocked current flow through 50% of the volume every few micrometers.

Since only a small number of cells can be simulated using this technique —usually only up to a few hundred cells— the geometrical model was designed to be a piece of a big slab of tissue with the simulated cluster being a 3D tile in an infinitely large piece of tissue replicating this tile in every direction. In order to assure a smooth fit among the tiles the program generating them was designed to match opposite borders, *e.g.* a cell crossing of the border of the simulation tile at one end will fit together with a cell cut in half by the border on the opposite side of the tile.

This geometrical model was used to compute the four effective bidomain conductivities (the intracellular and extracellular conductivities, along and transverse to the fiber direction). The values of these were calculated by applying an electrical field in a given direction (longitudinal or transverse) across the ICS or the ECS. All calculations were performed by assuming that the cell membrane does not conduct. Although there will be some current flow between both the ICS and ECS, the same approach was applied for the tissue under healthy conditions and resulted in values that are in good agreement with the effective intra- and extracellular conductivities as reported in literature [17]. The second reason for choosing an infinite resistance for the membrane model, is that the calculated values are intended to serve as a basis of a bidomain simulation. In the latter model the membrane is modeled separately and the two conductive spaces are assumed to be separated by an active membrane model which will include the passive component of the current leaking from one domain to the other.

The electrical field was applied by assuming a potential difference between opposing boundaries of the model. Hence the source was situated in the boundary condition. This boundary condition was used as well to assure that the simulated piece of tissue is part of a large piece of tissue. These two constraints led to the following boundary conditions:

(1) A current exiting at one boundary node has to enter the model at the opposite boundary node; and (2) the potential at a node of the boundary has to be equal to the potential of its counterpart on the opposite boundary, except for nodes on the boundaries perpendicular to the applied external field.

The effective conductivities were obtained by computing the total amount of current flowing through the piece of tissue in a certain direction. The latter was calculated using the finite element method using a mesh consisting of tetrahedrons that was created on top of the geometrical model. The effective conductivity is now computed as following:

$$\sigma_e = J_{ECS}/E_{app} \quad (1)$$

and,

$$\sigma_i = J_{ICS}/E_{app} \quad (2)$$

The solution to the finite element model was computed using an iterative solver. The model of the intracellular space consisted of approximately 1,4 million elements and the one of the extracellular space of 600,000 elements. The simulations were carried out in a cluster of 4 x 4 x 4 myocytes (a model of 64 cells) and the parameters chosen to represent the healthy condition are depicted in Table 1.

In the model all components are assumed to be ohmic and were assigned a conductivity value based on a literature survey. The interstitial conductivity was estimated at 2.0 S/m, which corresponds to the conductivity of many extracellular fluids in the body [8], [14] and as well to values derived from the chemical composition of the extracellular fluids [18]. The effective conductivity of the inside of myocyte was estimated at 0.3 S/m along the fiber direction and 0.15 S/m across. The latter values were estimated based the layout of myofibrils and mitochondria and the mobility of potassium in the remaining space of the cytoplasm [17]. This longitudinal conductivity value seems to agree with measurements performed by Brown *et al.* [2] when corrected for temperature. Since the model does not contain individual gap junction connections but models the effect of gap junctions by means of an effective surface resistance experienced between two cells, we had to estimate this effective surface resistance. We chose the effective gap junction surface resistivity to be 1 M Ω , spread out over half of the cross section of an average myocyte. This value was estimated based on the cell-to-cell resistances measured by Metzger and Weingart [12], [21] after correcting the value for the access resistance due to the resistance of the myocyte itself.

[INSERT TABLE 1 HERE]

In order to derive differences in the conductivity values between healthy and ischemic tissue, the parameters in the model need to be adapted to represent the tissue structure of ischemic tissue. The most prominent effect on the conductivity is the gradual closure of gap junctions. This effect was simulated by increasing the resistance of the cell-to-cell coupling in the model, from 1 M Ω coupling representing healthy tissue to 10 M Ω coupling, representing a partial closure of the gap junctions during ischemia. This value was chosen based upon observations by Jain *et al.*, who found that the density of gap junction proteins in a non preconditioned ischemia is somewhere between 10 to 20% of control values. Hence, we assumed around a tenfold increase in resistance of the surface resistance.

Besides the closure of gap junctions, morphological changes in the tissue structure may also affect the conductivity. During ischemia Kléber and Rieger [11] observed an abrupt decrease in extracellular myocardial conductivity. One way to explain this sudden increase is swelling of the capillaries (which conduct far more poorly than the extracellular medium due to red blood cells blocking the currents in the capillaries). Hence, we altered the size of the capillaries in the geometrical model, both swelling and collapse were simulated. Another influence on the myocardial conductivity is the swelling of myocytes during ischemia. We simulated this effect by changing the

size of the myocytes while keeping the spacing between the myocytes constant.

III. RESULTS

The results presented here were based on simulations in which we assumed the parameters depicted in Table 1 to represent the healthy/non-ischemic case. Using the parameters in Table 1, an effective intracellular conductivity of about 0.16 S/m (longitudinal) and 0.005 S/m (transverse), and an effective extracellular conductivity of about 0.21 S/m (longitudinal) and 0.05 S/m (transverse), was computed [17].

[INSERT FIGURE 2 HERE]

In order to predict the changes in the bidomain conductivities under ischemic conditions we performed three series of simulations under the following conditions: (1) an expansion of the capillaries in the ECS, (2) cell swelling, and (3) the closure of the gap junctions.

The first two of these simulation series mainly affected the bidomain conductivities in the extracellular space, shown in Figure 2. In the first simulation the capillaries were allowed to swell from a state in which they occupy about 30% of the ECS to a state in which they occupy 50% of the ECS. In the latter situation, the clusters of empty space surrounding the capillaries are gone and the interstitial volume is primarily made up out of the thin sheets of fluid that separate the myocytes. This is the largest volume fraction the capillary space can have in the model without affecting the spacing between myocytes. This increase of capillary volume leads to a noticeable reduction of the effective longitudinal extracellular conductivity and anisotropy ratio, but hardly affects the effective transverse extracellular conductivity. The conductivity was reduced from 0.21 S/m to a value of about 0.17 S/m a reduction by about 20%.

The second simulation series, shown in the bottom row of Figure 2, shows the effect of cell swelling. In this simulation the spacing between adjacent myocytes were held constant and the myocytes were allowed to swell leading to a reduction in the overall ECS volume fraction. In order to get noticeable effects in the conductivity of the extracellular conductivities, it was necessary for the myocytes to swell considerably, *e.g.* an increase of 50% in cell volume, leads to a 25% reduction of the extracellular conductivity.

In order to simulate the effect of gap junction closure we carried out various simulations in which the gap junction surface resistance was increased from 1 M Ω (healthy case) to a value 10 M Ω (ischemia). The latter increase only effected the intracellular conductivities which are depicted in Figure 3. The effective longitudinal and transverse conductivities decrease non-linearly with increases in the resistance of the gap junctions. Because the transverse conductivity is affected more by the increase of the gap junctional resistance than the longitudinal, the intracellular anisotropy factor increases as well. For cell-to-cell resistances over 10 M Ω , the gap junctional resistance becomes the dominate factor in both the transverse and the longitudinal effective intracellular conductivities resulting in an anisotropy factor in the range between 50 and 60 that is more or less independent of the value of

the gap junction resistance. The overall effect of a substantial increase in gap junction resistivity is a substantial drop in the intracellular conductivities and a rise in the ICS anisotropy ratio.

[INSERT FIGURE 3 HERE]

IV. DISCUSSION

One of the main motives for creating a model of cardiac conductivity was to estimate the changes in conductivity that arise during the various phases of ischemia. Experimental data regarding these changes is especially sparse. One problem encountered in estimating the conductivity of ischemic cardiac tissue is that ischemia is a cascade of different processes taking place over time so that there is no single static conductivity value for ischemic tissue. Hence, in relating the changes in cardiac conductivity to the underlying changes in physiological state, understanding these different stages and their implications becomes more important.

At the onset of ischemia, there is a sudden increase in the longitudinal extracellular conductivity [11], [15]. One hypothesis for this behavior is capillary swelling resulting from draining of the interstitial fluid out of the tissue after the loss of capillary hydrostatic pressure. In order to simulate this process, we simulated the swelling of the capillaries (Figure 2A), from a control state in which they occupied about 30% of the ECS to a state in which they occupied 50% of the ECS. In the latter condition, the capillaries filled the normally unoccupied space around them with only a minimal layer of interstitial fluid remaining between the capillaries and the myocytes. Simulations of this transition showed a reduction in the extracellular conductivity of about 20 to 25%, a value reasonably close to the measured reduction in the extracellular longitudinal conductivity of about 35% [11]. A more realistic response would be at least some drainage of interstitial fluid through the capillaries out of the ischemic region, and therefore somewhat less capillary swelling, but the next effect would still be a loss of interstitial fluid and hence the increased extracellular resistance.

The additional decrease in extracellular conductivity during the next phase of ischemia described by Smith *et al.* probably arises as a result of cell swelling [15]. We were able to replicate this small reduction in extracellular conductivity by allowing the cells in the model to swell by 8–16%, a reasonable range of values according to the literature [16], [19]. The decrease in conductivity in this phase was not as large as the one in the first phase, which seems to match the time curve of resistance in ischemia reported in literature [10], [11], [13], [15].

A further factor that influences tissue conductivity during ischemia is the reduction in the intracellular component that arises because of a graded failure in the gap junctions. To replicate the results of Smith *et al.*, which showed a two step rise in the longitudinal bulk resistivity of first 1.5 and then 2.7 fold, would require a decrease in the longitudinal bulk conductivity from 0.38 S/m to about 0.14 S/m. Given the reduction in conductivity for the extracellular space of some 40% described above, this would require a much larger

drop in the intracellular conductivity, which lies effectively in parallel with the extracellular conductivity. We simulated a tenfold increase in gap junction resistivity, which effectively made the extracellular conductivity the major contributor to the bulk conductivity. Under these conditions, the extracellular longitudinal conductivity was 0.13 S/m and the intracellular was 0.03 S/m, resulting in a bulk longitudinal conductivity of 0.16 S/m, which is close to the 0.14 S/m value observed by Smith *et al.* [15]. The actual increase of the gap junction resistivity is hard to estimate from current literature. However, a recent study by Jain *et al.* [10] showed that when cardiac tissue is subjected to 30 minutes of no flow ischemia, the density of connexin-43 proteins in the cell membranes was reduced to 10–20% of the original density. This tenfold decrease can be correlated to the tenfold increase of the cell-to-cell resistance.

We did not include the well documented effect of elevated extracellular potassium concentration in the simulations of ischemic conductivity. Even with a typical elevation of potassium, the dominant extracellular ions remain sodium and chloride such that the effect on electrolyte conductivity is likely to be negligible (less than 5%).

ACKNOWLEDGMENT

This research would not have been possible without the generous support of the National Institutes of Health BISTI Grant P20 HL68566-01.

REFERENCES

- [1] M. A. Beardslee, L. D. Lerner, P. N. Tadros, J. G. Laing, E. C. Beyer, K. A. Yamada, A. G. Kleber, R. B. Schuessler, and J. E. Saffitz. Dephosphorylation and Intracellular Redistribution of Ventricular Connexin43 During Electrical Uncoupling Induced by Ischemia. *Circ. Res.*, 87:656–662, 2000.
- [2] A. M. Brown, K. S. Lee, and T. Powell. Voltage clamp and internal perfusion of single rat heart muscle cells. *J. Physiol.*, 318:455–477, 1981.
- [3] E. Carmeliet. Cardiac Ionic Currents and Acute Ischemia: From Channels to Arrhythmias. *Physiol. Rev.*, 79(3):917–1017, 1999.
- [4] J. Cinca, M. Warren, A. Carreno, M. Tresanchez, L. Armadans, P. Gomez, and J. Soler-Soler. Changes in myocardial electrical impedance induced by coronary artery occlusion in pigs with and without preconditioning. *Circ.*, 96:3079–3086, 1997.
- [5] H. S. Duffy, A. W. Ashton, P. O'Donnell, W. Coombs, S. M. Taffet, M. Delmar, and D. C. Spray. Regulation of Connexin43 Protein Complexes by Intracellular Acidification. *Circ. Res.*, 94:215–222, 2004.
- [6] J. Fleischhauer, L. Lehmann, and A. G. kleber. Electrical resistances of interstitial and microvascular space and determinants of the extracellular electrical field and velocity of propagation in ventricular myocardium. *Circ.*, 92(3):587–594, 1995.
- [7] M.S. Forbes and N. Sperelakis. Chapter 1 - Ultrastructure of mammalian cardiac muscle. In *Physiology and pathophysiology of the heart*, pages 1–35. Kluwer Academic Publishers, Norwell MA, 3rd edition, 1995.
- [8] K. R. Foster and H. P. Schwan. Dielectric properties of tissues and biological materials: a critical review. *Crit. Rev. Biomed. Eng.*, 17(1):25–104, 1989.
- [9] B. Hopenfeld, J. G. Stinstra, and R. S. Macleod. A Mechanism for ST Depression Associated with Contiguous Subendocardial Ischemia. *Accepted for publication in J. Cardiovasc. Electrophysiol.*, 2004.
- [10] S. K. Jain, R. B. Schuessler, and J. E. Saffitz. Mechanisms of delayed electrical uncoupling induced by ischemic preconditioning. *Circ. Res.*, 92(10):1138–1144, 2003.
- [11] A. G. Kléber and C. B. Riegger. Electrical constants of arterially perfused rabbit papillary muscle. *J. Physiol.*, 385:307–324, 1987.
- [12] P. Metzger and R. Weingart. Electric current flow in cell pairs isolated from adult rat hearts. *J. Physiol.*, 366:177–195, 1985.
- [13] LM Owens, TA Fralix, E Murphy, WE Cascio, and LS Gettes. Correlation of Ischemia-Induced Extracellular and Intracellular Ion Changes to Cell-to-Cell Electrical Uncoupling in Isolated Blood-Perfused Rabbit Hearts. *Circ.*, 94:10–13, 1996.
- [14] H. P. Schwann and C. F. Kay. The conductivity of living tissues. *Ann. N.Y. Acad. Sci.*, 65:1007–1013, 1956.
- [15] W. T. Smith, W. F. Fleet, T. A. Johnson, C. L. Engle, and W. E. Cascio. The Ib phase of ventricular arrhythmias in ischemic in situ porcine heart is related to changes in cell-to-cell electrical coupling. *Circ.*, 92:3051–3060, 1995.
- [16] C Steenbergen, ML Hill, and RB Jennings. Volume regulation and plasma membrane injury in aerobic, anaerobic, and ischemic myocardium in vitro. *Circ. Res.*, 57:864–875, 1985.
- [17] J. G. Stinstra, B. Hopenfeld, and R. S. MacLeod. On the passive cardiac conductivity. *submitted to ABME*, 2005.
- [18] J. G. Stinstra and M. J. Peters. The influence of fetoabdominal tissues on fetal ECGs and MCGs. *Arch. Physiol. Biochem.*, 110(3):165–176, 2002.
- [19] J. Tranum-Jensen, M. J. Janse, J. W. T. Fiolet, W. J. G. Krieger, C. N. D'Alnoncourt, and D. Durrer. Tissue Osmolality, Cell Swelling, and Reperfusion in Acute Regional Myocardial Ischemia in the Isolated Porcine Heart. *Circ. Res.*, 49:364–381, 1981.
- [20] E. D. Trautman and R. S. Newbower. A practical analysis of the electrical conductivity of blood. *IEEE Trans. Biomed. Eng.*, 30(3):141–153, 1983.
- [21] R Weingart. Electrical properties of the nexal membrane studied in rat ventricular cell pairs. *J Physiol*, 370:267–84, 1986.
- [22] A. R. Wright and S. A. Rees. Cardiac cell volume: crystal clear or murky waters? A comparison with other cell types. *Pharmacol. Ther.*, 80(1):89–121, 1998.
- [23] G. X. Yan, J. Chen, K. A. Yamada, A. G. Kleber, and P. B. Corr. Contribution of Shrinkage of Extracellular Space to Extracellular K⁺ Accumulation in Myocardial Ischemia of the Rabbit. *J. Physiol.*, 490.1(3):215–228, 1996.

TABLE 1
OVERVIEW OF THE PARAMETERS USED IN THE CONDUCTIVITY MODEL
(HEALTHY TISSUE)

Parameter	Value
Cytoplasm longitudinal conductivity	0.3 S/m
Cytoplasm transverse conductivity	0.15 S/m
Interstitial conductivity	2.0 S/m
Capillary wall conductivity	0.02 S/m
Blood plasma conductivity	2.0 S/m
Haematocrit	50 %
Gap-junction resistivity	$1.45 \cdot 10^{-4} \Omega\text{m}^2$
Cell membrane resistivity	$+\infty \Omega\text{m}^2$
Average cell cross-section	$300 \mu\text{m}^2$
Average cell length	$95 \mu\text{m}$
Volume fraction myocytes	84 %
Volume fraction interstitial space	11 %
Volume fraction capillaries	5 %

FIGURE CAPTIONS

FIGURE 1

The process used to create a geometric model of cardiac tissue. The process starts with building a random cross section of a myocyte out of hexagons. Subsequently more hexagons are added to form a full cross section. In this process, capillaries are assigned as well which are interspersed with the myocytes. In the next phase a certain amount of extracellular space is added in between the myocytes and the myocytes are given a third dimension by extending the hexagonal column in the fiber direction. As the latter process is random the resulting myocyte shapes have the spiky look often found in microscopic images. Finally, the more layers are added to form a full 3D model of a piece of cardiac tissue. The arrangement of gap junctions associated with a single myocyte, is depicted in the lower illustration. All the faces perpendicular to the fiber direction are assumed to contain gap junctions and in the model these faces touch the next layer of cells, assuring a cell-to-cell conduction through the intracellular space

FIGURE 2

Effective extracellular conductivity as a function of changes in the morphology of the ECS. The upper row depicts the changes due to respectively capillary swelling and the collapse of capillaries; the lower row depicts the effect of myocyte swelling.

FIGURE 3

Effective intracellular conductivity as a function of the average myocyte length, average myocyte cross-section, cytoplasm conductivity, and the gap junction cell-to-cell resistance. The first column displays the longitudinal effective conductivity, the second the effective transverse conductivity, and the third the anisotropy ratio. In each of the graphs only one parameter is varied. The other parameters are kept at the following reference values: $95 \mu\text{m}$ for the average myocyte length, $300 \mu\text{m}^2$ for the average myocyte cross section, and 0.3 S/m for the effective cytoplasm conductivity. For the cell-to-cell resistance, two values were chosen, $1 \text{ M}\Omega$ for healthy tissue (solid line) and $10 \text{ M}\Omega$ for ischemic tissue (dashed line). The simulations shown in this graph were repeated ten times with different geometrical layouts of the cells in the cluster. The error bars indicate the maximum and minimum values found for the effective conductivities. Note that the error bars for the longitudinal case are tiny.

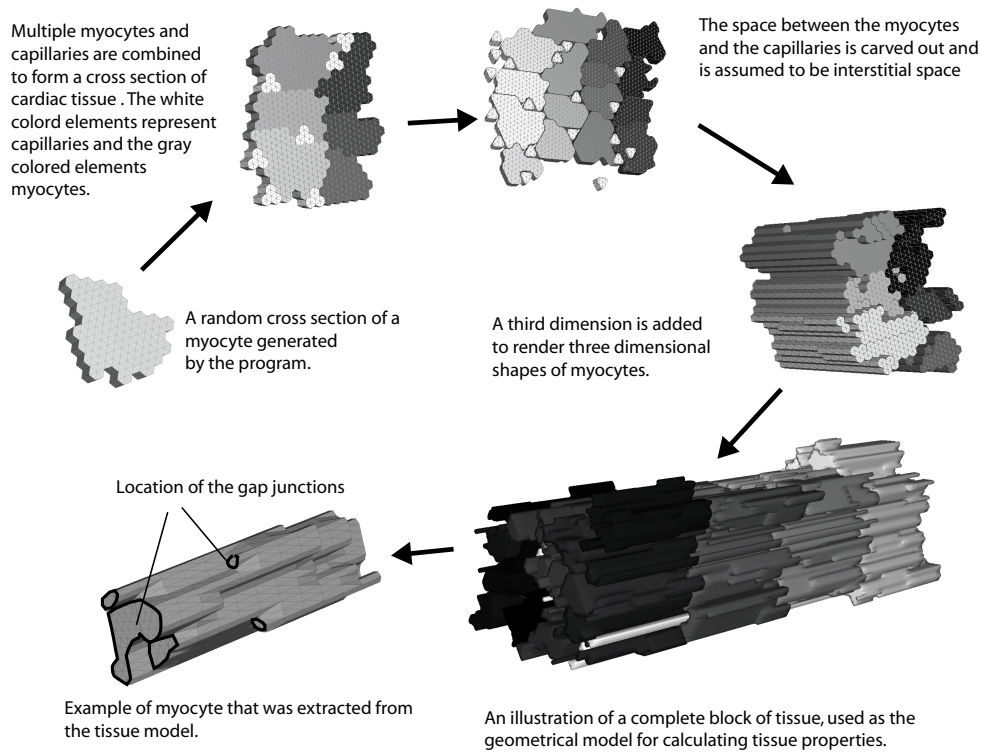


Fig. 1.

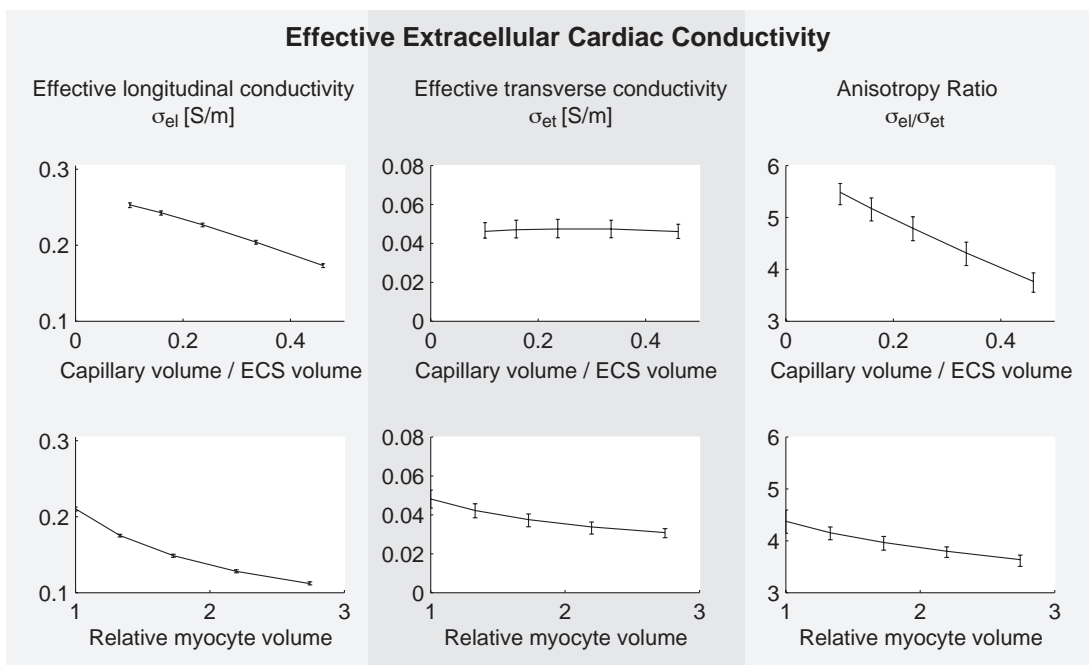


Fig. 2.

Effective Intracellular Cardiac Conductivity

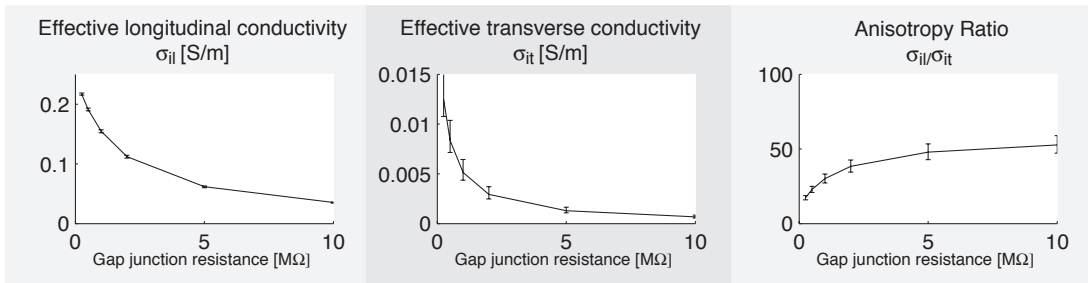


Fig. 3.